ISSN 0029-3865

CBPF- CENTRO BRASILEIRO DE PESQUISAS FÍSICAS

Notas de Física

FERMILAB-Pub-92/208-E
CBPF-NF-034/92

FEYNMAN-x AND TRANSVERSE MOMENTUM DEPENDENCE OF $D^{\pm}$ AND D^0, $\bar{D}^0$ PRODUCTION IN 250 GEV π^- - NUCLEON INTERACTIONS

by

G.A. ALVES, S. AMATO, J.C. ANJOS, J.A. APPEL,
S.B. BRACKER, L.M. CREMALDI, C.L. DARLING, R.L. DIXON,
D. ERREDE, H.C. FENKER, C. GAY, D.R. GREEN, R. JEDICKE,
D. KAPLAN, P.E. KARCHIN, S. KWAN, I. LEEDOM, L.H. LUEKING,
G.J. LUSTE, P.M. MANTSCH, J.R.T. de MELLO NETO, J. METHENY,
R.H. MILBURN, J.M. de MIRANDA, H. da MOTTA FILHO,
A. NAPIER, A.B. d'OLIVERA, A. RAFATIAN, A.C. dos REIS,
S. REUCROFT, W.R. ROSS, A.F.S. SANTORO, M. SHEAFF,
M.H.G. SOUZA, W.J. SPALDING, C. STOUGHTON, M.E. STREETMAN,
D.J. SUMMERS, S.F. TAKACH and Z. WU

We measure the differential cross-section with respect to Feynman-x (x_F) and transverse momentum (P_T) for charm meson production using targets of Be, Al, Cu and W. In the range $0.1 < x_F < 0.7$, $d\sigma/dx_F$ is well fit by the form $(1 - x_F)^n$ with $n = 3.9 \pm 0.2$. The difference between n values for D^- and D^+ is 1.1 ± 0.4. However, we find an asymmetry of 0.18 ± 0.04 favoring the production of D^- compared to D^+. In the lower P_T range, < 2 GeV, $d\sigma/dP_T^2$ is well fit by the form $\exp(-b \times P_T^2)$ with $b = 1.03 \pm 0.04$ GeV^{-2}, while in the higher P_T range, 0.8 to 3.6 GeV, it is well fit by the form $\exp(-b' \times P_T)$ with $b' = 2.76 \pm 0.06$ GeV^{-1}. The shape of the differential cross-section has no significant dependence on atomic mass of the target material.

PACS numbers: 12.38.Qk, 13.85.Ni

Although charm was co-discovered using hadronic interactions in 1974, the production mechanism is still not well established. In perturbative QCD, charm is hadroproduced by gluon-gluon fusion and quark-anti-quark annihilation. The total and differential cross sections for charm quark production have been calculated using perturbative QCD by Nason, Dawson, and Ellis (NDE) including terms up to next-to-leading order (NLO) [1]. Some measurements [2, 3] of total cross-section and differential cross section in x_F and P_T are consistent with the NDE predictions. However, other experiments [4–7] report either a total cross section larger than can be accommodated by NLO QCD and/or show large differences in the production of leading versus non-leading charm. (Leading charm particles have at least one valence quark that was transferred from the projectile.) To explain some of these measurements, Combridge [8] and Brodsky *et al.* [9] postulated production from the charm component of the parton sea of hadrons.

Fermilab experiment E769 addresses these issues with a high statistics study of exclusively reconstructed charm particles using 250 GeV secondary beams with identified $\pi^{\pm}$, $K^{\pm}$ and p on thin foil targets of Be, Al, Cu and W. The data were collected during the 1987-88 running period. In this letter we report differential cross-sections measured using the decays $D^+ \rightarrow K^-\pi^+\pi^+$ and $D^0 \rightarrow K^-\pi^+$ (and charge conjugates). Results on the total charm cross-section and the dependence on atomic mass and incident particle type are in preparation.

The open-geometry spectrometer used in E769 was substantially the same as previously used in Fermilab photo-production experiment E691 [10]. For E769, the spectrometer included an 11-plane silicon microstrip (SMD) vertex detector, 2 analyzing magnets, 35 drift chambers, 2 multi-wire proportional chambers (MWPC's), 2 segmented, threshold Cerenkov counters, calorimeters, a muon detector, and a high-rate, microprocessor-based data acquisition system. For beam particle identification we used a differential Cerenkov counter (DISC) and a transition radiation detector, the latter used for data taken with a positively charged beam. For beam tracking we used 8 MWPC's and 2 SMD's.

More detailed descriptions of the apparatus are found in [11] and references quoted therein.

With the DISC set to tag kaons, the beam sample used in this analysis consisted of 94% π^- with a contamination of 4.0 K^- and 2% $\bar{p}$. The trigger required total transverse energy in the calorimeters > 5.5 GeV. This reduced the event rate by a factor of 3 while maintaining an efficiency of about 75% for charm. About 400 million events were recorded in the entire data set, 150 million of these from π^- interactions.

In off-line analysis we reconstructed the complete data sample. The analysis for charged tracks included pattern recognition, fitting, vertex reconstruction, and particle identification. We reduced the event sample by a factor of 14 by selecting events which had a pair of tracks forming a downstream vertex and whose separation from the primary vertex had a significance of at least 6 standard deviations (6σ).

We applied further analysis cuts to select events with either the charged or neutral decay. The significance of the vertex separation was required > 12σ (6σ) for charged (neutral) decays. The direction of the D was calculated from the summed three-momenta of the decay products. The summed P_T^2 of the decay tracks, with P_T measured relative to the direction of the parent, was required > 0.5 GeV^2 (0.7 GeV^2) for charged (neutral) decays. For neutral decays, the product of the summed P_T^2 and the significance of the vertex separation was required > 11 GeV^2. The distance between the primary vertex and the line of flight of the parent D was required < 80 μm (100 μm) for charged (neutral) decays. The minimum of the set of distances from the decay vertex to each track not in the decay vertex was required > 60 μm for charged decays. We calculated the product over the decay tracks of terms which, for each decay track, is the ratio of its' distance from the secondary vertex to its' distance from the primary vertex. This product was required < 0.006 (0.1) for charged (neutral) decays. Using the Cerenkov counters, we excluded identified pions as candidate kaons from charm decay. The resulting invariant mass plots for the two decay channels are shown in Fig. 1.

We performed a binned maximum likelihood fit to these mass plots using a gaussian signal and a linear background. The widths were fixed according to the Monte Carlo simulation. The number of signal events is 700 ± 24 for the charged D and 607 ± 29 for the neutral D. To determine the differential distributions, we made a mass plot for each bin of x_F and P_T and fit them as previously described. The gaussian widths are independent of P_T but range from 9 MeV at low x_F to 16 MeV at high x_F.

The acceptance was calculated from a complete Monte Carlo simulation which included the effects of the resolution, geometry and efficiency of all detectors, interactions in the apparatus, and all analysis cuts. The event generator used a leading order (LO) QCD calculation for the charm quark pair, FRITIOF version 1.3 [13] to simulate the underlying interaction, and JETSET version 6.3 [12] to hadronize the partons. The acceptance for charged and neutral D's is similar. As a function of x_F, it varies between 2% and 6% in the range 0.0 to 0.8 with a maximum at 0.25. The acceptance in P_T increases from 4% to 8% over the range 0 to 4 GeV. Systematic errors in the acceptance include the uncertainties in trigger simulation and detector efficiencies. The systematic errors are small compared to statistical errors in the data and thus we quote only one error (statistical) in our results.

Our measured $d\sigma/dx_F$ for charged and neutral particles combined is shown in Fig. 2. We performed a least-squares fit to the data using the functional form $(1-x_F)^n$ which gives a good fit in the range $0.1 \leq x_F \leq 0.7$ with $n = 3.9 \pm 0.2$. We also show the prediction of NDE for charm quark production for a quark mass of 1.5 GeV, scaled to the data. A fit to these theory points over the same range yields $n = 4.25$. While the prediction matches the data well, we note that the effect of fragmentation of the quarks into mesons is not taken into account in the calculation of NDE.

Our results for combined charged and neutral D's are compared with those from other experiments in Table II. Our values of n are consistent with those measured in NA32 [2] but our value for the difference in n between leading and non-leading charm (0.3 ± 0.4) does not confirm the large difference suggested by the NA27 measurement of (6.1 ± 1.5) [7]. To best test for a leading particle effect versus x_F, we analyzed our x_F dis-

tributions separately for D^- (leading) and D^+ (non-leading). We chose charged D's because the leading/non-leading character is the same whether the charged D is directly produced or results from the decay of a D^*, while this is not the case for the neutral D's. We measure $n(D^+) - n(D^-) = 1.1 \pm 0.4$.

We further test for a leading particle effect by calculating the asymmetry, $A(x,y) = [\sigma(x) - \sigma(y)]/[\sigma(x) + \sigma(y)]$, where $\sigma(x)$ is the number of events with meson x divided by the acceptance for meson x, as a function of x_F, integrated over $x_F > 0$. We obtain $A(D^-, D^+) = 0.18 \pm 0.04$ and $A(D^0, \overline{D}^0) = -0.06 \pm 0.05$. Thus we see a 4.5σ asymmetry in the charged D channel but no effect in the neutral channel.

Our results for $d\sigma/dP_T^2$ are plotted in Fig. 3. At high P_T (> 2 GeV) there is a significant deviation from the functional form $\exp(-b \times P_T^2)$, an effect not seen in experiments with smaller statistics. To compare our measurement with those from other experiments, we fit our data to the above form in a limited range as shown in Fig. 3 and in the tables.

For $P_T > 0.8$ GeV, $d\sigma/dP_T^2$ is well fit by the form $\exp(-b' \times P_T)$. This is shown in Fig. 4 which also shows the prediction for charm quarks using LO QCD [14]. This is also well fit with the same functional form. In addition to the previous requirement, $P_T > 0.8$ GeV, we restrict the fit range to $P_T < 2.4$ GeV so that we can compare b' values for various sub-samples, which were measured with lower statistics, as given in Table I. Fitting the theory points in the same range yields $b' = 2.16$ GeV^{-1}. For the full sample we use the larger range $0.8 < P_T < 3.6$ GeV to obtain our best value of $b' = 2.76 \pm 0.06$ GeV^{-1}.

If charm production is due to short distance collisions and fragmentation, then there should be little dependence of the x_F, P_T, or P_T^2 distributions on the atomic mass of the target material. To test this hypothesis, we fit these distributions separately for Be, Al, Cu and W. The values of n, b' and b are given in Table I. We see no significant dependence of these parameters on atomic mass.

This research was supported by the U.S. Department of Energy, the U.S. National Science Foundation, the Brazilian Conselho Nacional de Desenvolvimento Científico e Tecnológico, and the National Research Council of Canada.

FIG. 1. Invariant mass distribution for (left plot) $D^+ \to K^-\pi^+\pi^+$ (+ c.c.) and (right plot) $D^0 \to K^-\pi^+$ (+ c.c.).

FIG. 2. Measured $d\sigma/dx_F$ and comparison with the NLO QCD prediction for quarks [1]. The arrow indicates 90% C.L. upper limit. The solid (dashed-dotted) curve is from a fit to the measurements (theory) over the range 0.1 to 0.7, and the dashed (dotted) curve shows the extrapolation of this fit over the full range.

FIG. 3. Measured $d\sigma/P_T^2$ versus P_T^2 and a fit over the range 0 to 4 GeV^2 (solid curve), extrapolated to the full range (dashed curve). The arrows indicate 90% C.L. upper limits.

FIG. 4. Measured $d\sigma/P_T^2$ versus P_T and comparison with the LO QCD prediction for quarks [14]. The solid (dashed-dotted) curve is a fit to the measurements (theory) over the range 0.8 to 2.4 GeV, and the dashed (dotted) curve shows the extrapolation of this fit over the full range.

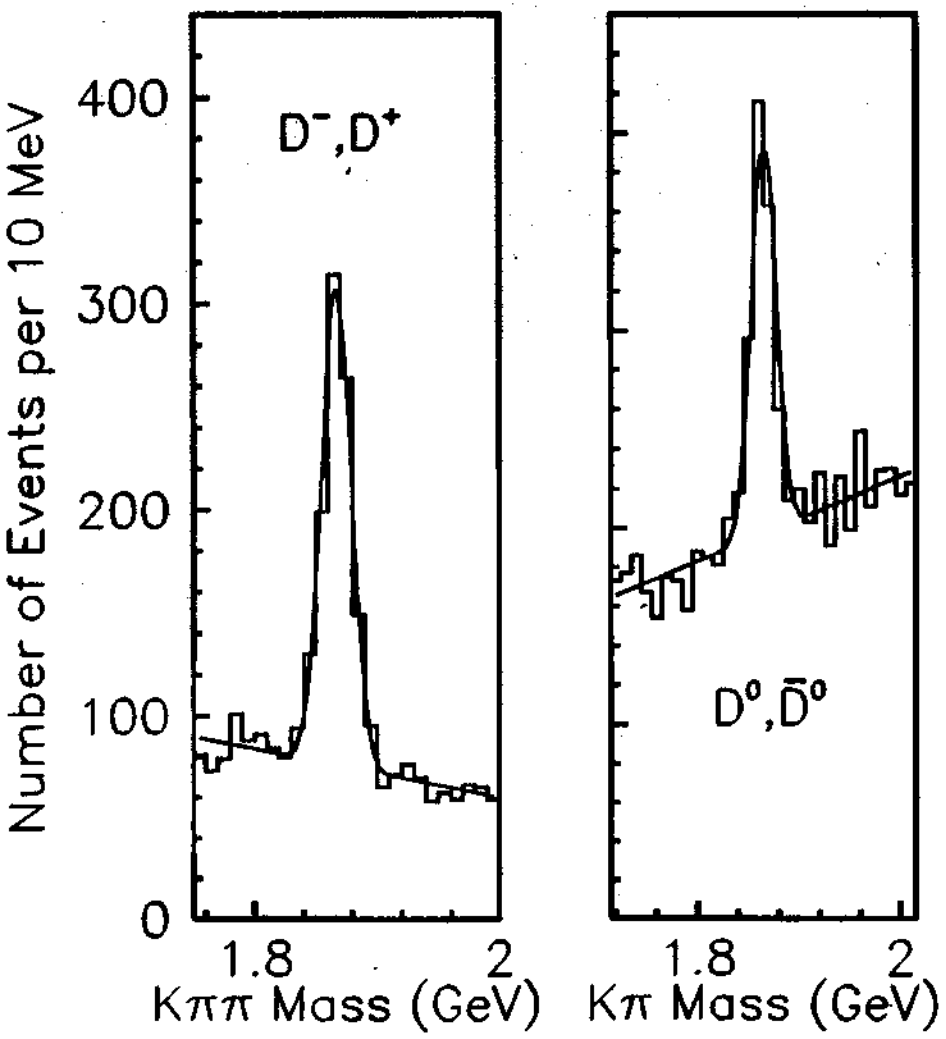
Number of Events per 10 MeV
400
300
200
100
0
D⁻,D⁺
D⁰,D̄⁰
1.8
2
Kππ Mass (GeV)
1.8
2
Kπ Mass (GeV)

Figure 1

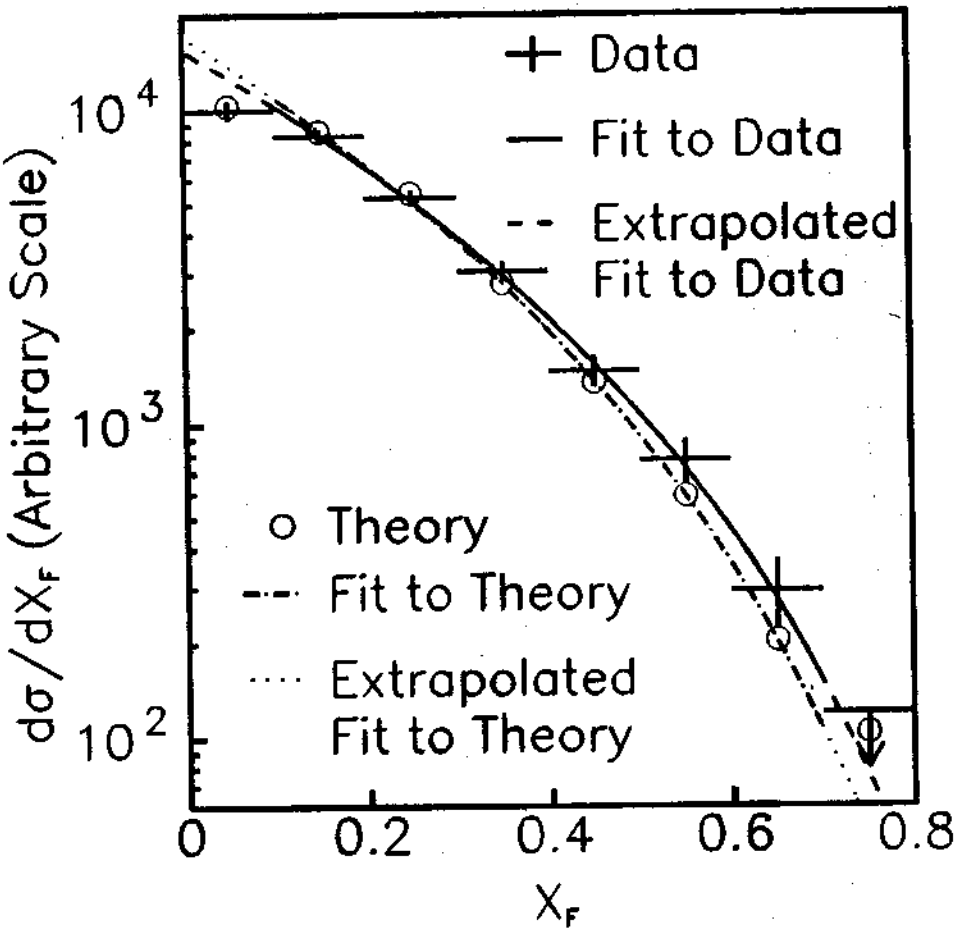
Data
Fit to Data
Extrapolated
Fit to Data
Theory
Fit to Theory
Extrapolated
Fit to Theory
10^4
10^3
10^2
$d\sigma/dX_F$ (Arbitrary Scale)
0
0.2
0.4
0.6
0.8
X_F

Figure 2

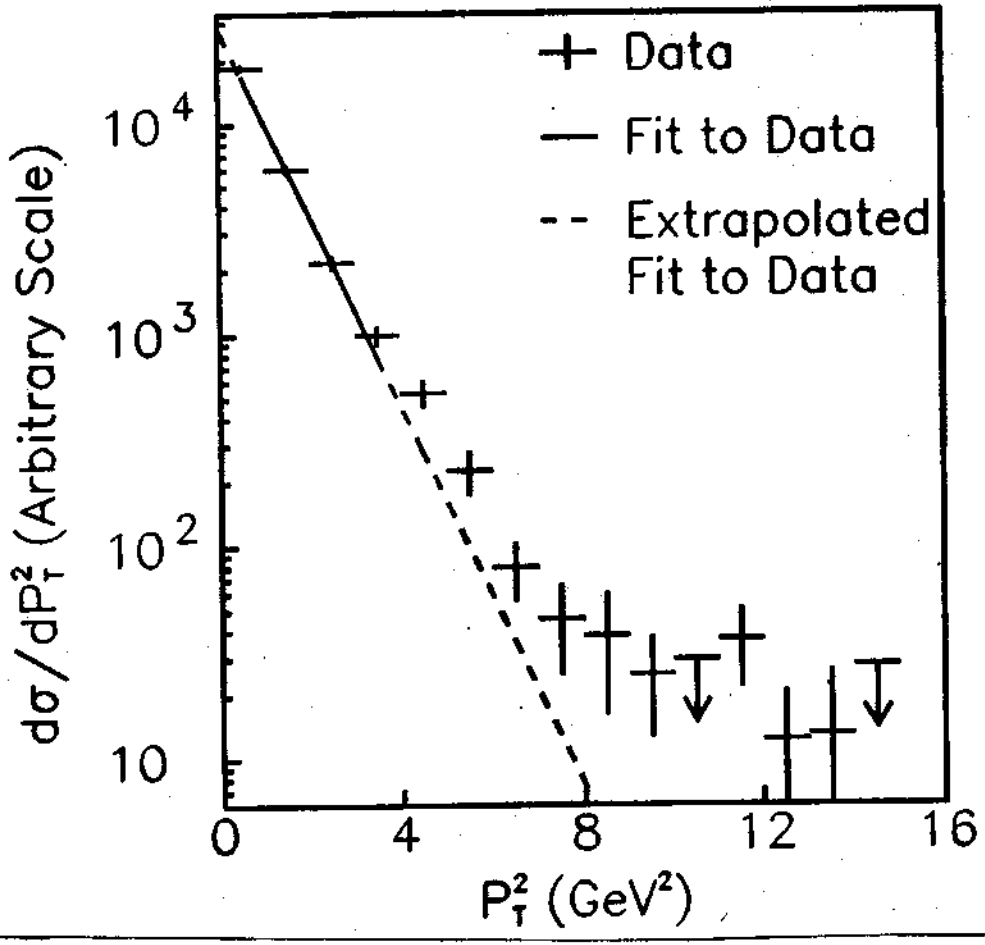
Data
Fit to Data
Extrapolated
Fit to Data
10^4
10^3
10^2
10
$d\sigma/dP_T^2$ (Arbitrary Scale)
0
4
8
12
16
P_T^2 (GeV^2)

Figure 3

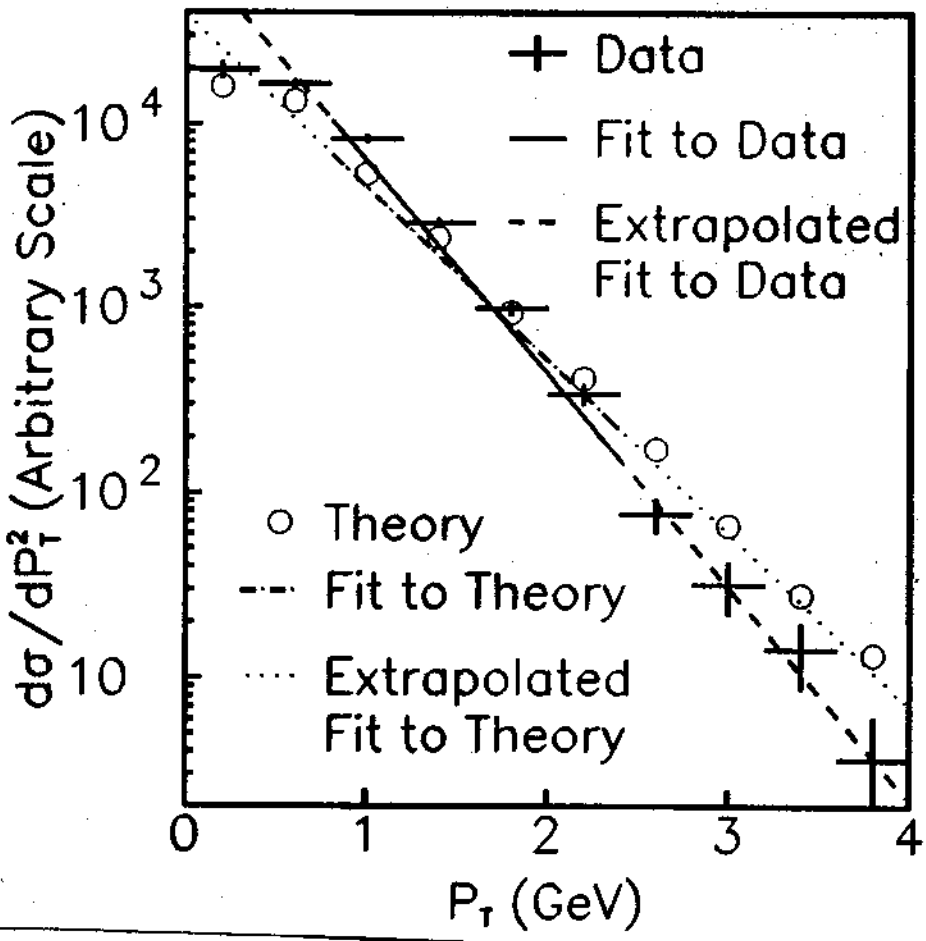
Data
Fit to Data
Extrapolated
Fit to Data
Theory
Fit to Theory
Extrapolated
Fit to Theory
$d\sigma/dP_T^2$ (Arbitrary Scale)
10^4
10^3
10^2
10
0
1
2
3
4
P_T (GeV)

Figure 4

TABLE I. Production parameters (described in the text) from fits to E769 data. Errors quoted are statistical only since systematic errors are small in comparison. Values and errors are rounded off to the number of decimal places shown.

Fit Range		$0.1 < x_F < 0.7$	$0.0 < P_T^2 < 4.0$ GeV^2	$0.8 < P_T < 2.4$ GeV
Target	Meson	n	b (GeV^{-2})	b' (GeV^{-1})
All	$D^+,D^-,D^0,\overline{D}^0$	3.9 ± 0.2	1.03 ± 0.04	2.66 ± 0.08
All	D^-,D^0	3.7 ± 0.3	1.07 ± 0.05	2.67 ± 0.11
All	$D^+,\overline{D}^0$	4.0 ± 0.3	0.99 ± 0.05	2.66 ± 0.12
All	D^-	3.3 ± 0.3	1.05 ± 0.14	2.67 ± 0.13
All	D^+	4.4 ± 0.3	0.92 ± 0.06	2.55 ± 0.15
All	D^+,D^-	3.7 ± 0.2	0.99 ± 0.04	2.62 ± 0.10
All	$D^0,\overline{D}^0$	4.2 ± 0.3	1.08 ± 0.06	2.72 ± 0.14
Be	$D^+,D^-,D^0,\overline{D}^0$	3.7 ± 0.6	1.11 ± 0.11	3.07 ± 0.23
Al	$D^+,D^-,D^0,\overline{D}^0$	3.2 ± 0.4	0.97 ± 0.08	2.52 ± 0.21
Cu	$D^+,D^-,D^0,\overline{D}^0$	4.7 ± 0.4	1.18 ± 0.06	3.18 ± 0.19
W	$D^+,D^-,D^0,\overline{D}^0$	4.2 ± 0.4	1.04 ± 0.08	2.05 ± 0.23

TABLE II. Production parameters for incident π^- and for neutral and charged D mesons, combined, from this experiment compared to other measurements.

Expt.	E769	NA32	NA27
P_{beam} (GeV)	250	230	360
Target(s)	Be, Al, Cu, W	Cu	H
x_F Fit Range	0.1 to 0.7	0.0 to 0.8	0.0 to 0.9
n(all)	3.9±0.2	$3.74 \pm 0.23 \pm 0.37$	3.8±0.63
$n(D^-, D^0)$	3.7±0.3	$3.23^{+0.30}_{-0.28} \pm 0.32$	$1.8^{+0.6}_{-0.5}$
$n(D^+, \overline{D}^0)$	4.0±0.3	$4.34^{+0.36}_{-0.35} \pm 0.43$	$7.9^{+1.6}_{-1.4}$
Fit Range in P_T^2 (GeV^2)	0 to 4	0 to 10	0 to 4.5
b(all)(GeV^{-2})	1.03±0.04	$0.83 \pm 0.03 \pm 0.02$	$1.18^{+0.18}_{-0.16}$
$b(D^-, D^0)$	1.07±0.05	$0.74 \pm 0.04 \pm 0.02$	
$b(D^+, \overline{D}^0)$	0.99±0.05	$0.95 \pm 0.05 \pm 0.03$	

[1] P. Nason, S. Dawson, K. Ellis, Nucl. Phys. **B327**, 49 (1989).

[2] ACCMOR Collaboration, S. Barlag *et al.* Z. Phys. **C49**, 555 (1991).

[3] LEBC-MPS Collab., R. Ammar *et al.*, Phys. Rev. Lett. **61**, 2185 (1988).

[4] K.L. Giboni *et al.*, Phys. Lett. **85B**, 437 (1979).

[5] R608 Collab., P. Chauvat *et al.*, Phys. Lett. **199B**, 304 (1987).

[6] E400 Collab., C. Shipbaugh *et al.*, Phys. Rev. Lett. **60**, 2117 (1988).

[7] NA27 LEBC-EHS Collab., M. Aguilar-Benitez *et al.*, Phys. Lett. **161B**, 400 (1985); **201B**, 176 (1988).

[8] B.L. Combridge, Nucl. Phys. **B151**, 429, (1979).

[9] S.J. Brodsky *et al.*, Phys. Lett. **93B**, 451 (1980).

[10] E691 Collab., J.R. Raab *et al.*, Phys. Rev. **D 37**, 2391 (1988).

[11] P. Karchin and Z. Wu, in proc. of *3rd Topical Seminar on Heavy Flavors*, San Miniato (1991), Nucl. Phys. **B**, Proc. Supplements Section (to be published); R. Jedicke and L. Lueking, in proc. of *The Vancouver Meeting - Particles and Fields '91*, D. Axen *et al.* ed., World Scientific, 690 (1992); C. Stoughton and D.J. Summers, Computers in Physics **6**, 371 (1992); Z. Wu, Ph.D. thesis, Yale Univ., 1991 (unpublished); R. Jedicke, Ph.D. thesis, Univ. of Toronto, 1991 (unpub.); C. Gay, Ph.D. thesis, Univ. of Toronto, 1991 (unpub.); J.R.T. de Mello Neto, Ph.D. thesis, Centro Brasileiro de Pesquisas Físicas, 1992 (unpub.).

[12] T. Sjöstrand, Comput. Phys. Commun. **39**, 347 (1986).

[13] B. Nilsson-Almqvist and E. Stenlund, Comput. Phys. Commun. **43**, 387 (1987).

[14] K. Ellis, in proc. of *Les Rencontres de Physique de la Vallée d'Aoste: Results and Perspectives in Particle Physics*, M. Greco, ed., Editions Frontieres, 187 (1987).